ACS Catalysis

pubs.acs.org/acscatalysis Letter

Copper-Catalyzed Enantioselective Borylative Allyl−Allyl Coupling of Allenes and Allylic *gem*-Dichlorides

Martín Piñeiro-Suárez, Andrés M. Álvarez-Constantino, and Martín Fañanás-Mastral*

Cite This: *ACS Catal.* 2023, 13, 5578−5583 Read Online

ACCESS | Metrics & More | Article Recommendations | Supporting Information

ABSTRACT: A catalytic asymmetric reaction between allenes, bis(pinacolato)diboron, and allylic *gem*-dichlorides is reported. The method involves the coupling of a catalytically generated allyl copper species with the allylic *gem*-dichloride and provides chiral internal 1,5-dienes featuring (*Z*)-configured alkenyl boronate and alkenyl chloride units with high levels of chemo-, regio-, enantio-, and diastereoselectivity. The synthetic utility of the products is demonstrated with the synthesis of a range of optically active compounds. DFT calculations reveal key noncovalent substrate−ligand interactions that account for the enantioselectivity outcome and the diastereoselective formation of the (*Z*)-alkenyl chloride.

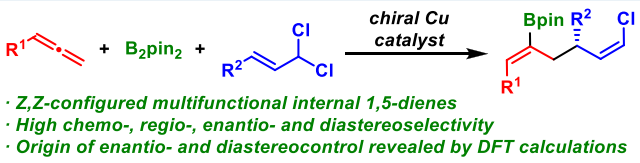

KEYWORDS: *copper, allylboration, asymmetric catalysis, allenes, multifunctional compounds, noncovalent interactions*

Downloaded via UNIV DE SANTIAGO DE COMPOSTELA on October 31, 2023 at 12:58:09 (UTC).
See https://pubs.acs.org/sharingguidelines for options on how to legitimately share published articles.

Catalytic asymmetric transformations that provide control over several stereochemistry elements in a single operation are among the most important challenges in modern organic chemistry.[1] Asymmetric allyl−allyl coupling of unsymmetrical allyl compounds represents an especially challenging type of reaction since, besides control over the enantioselectivity, many different regio- and stereoisomers can originate from coupling at either the α or γ position of both allylic reagents (Scheme 1a). Enantioselective allyl−allyl coupling has been achieved through Pd-,[2] Cu-,[3] and Ir-catalyzed[4] coupling of stoichiometric allyl metal reagents with several allylic electrophiles. However, these methods are typically confined to the introduction of simple allyl fragments from allyl metal reagents, and are limited to the synthesis of terminal 1,5-dienes (Scheme 1b).[5,6]

An interesting alternative to the stoichiometric use of allyl metal reagents in cross-coupling reactions is the catalytic generation of an allyl copper nucleophile by allene element-cupration.[7] By using this strategy, Hoveyda et al. reported a regio- and enantioselective borylative allyl−allyl coupling between allenes and primary allylic phosphates (Scheme 1c).[8] Additionally, Xiong et al.[9] and Hoveyda et al.[10] described the reductive version of this coupling by using copper hydride catalysis. Despite these efforts, the use of secondary 1,3-disubstituted allyl electrophiles in enantioselective allyl−allyl cross-coupling, which imposes an extra selectivity challenge since the geometry of the resulting internal double bond must be controlled, is elusive.[5] As far as we are aware, only one racemic example of a borylative allyl−allyl coupling involving a 1,3-disubstituted allyl phosphate has been reported.[11]

Within our ongoing interest in developing enantioselective multicomponent couplings of allylic *gem*-dichlorides,[12,13] we envisioned that an enantioselective allene allylboration based on this type of allylic substrates would afford an unprecedented

Scheme 1. Enantioselective Allyl−Allyl Cross-Coupling

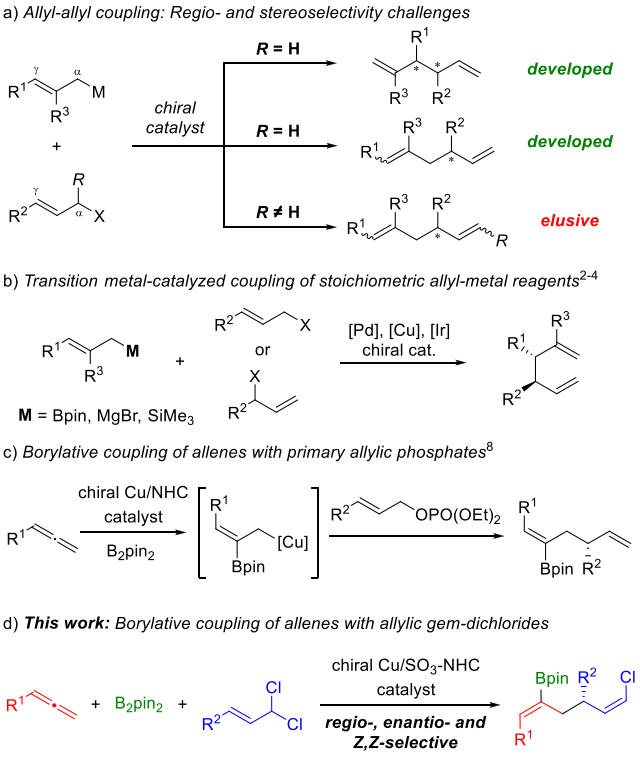

Received: February 3, 2023
Revised: April 3, 2023
Published: April 10, 2023

ACS Publications © 2023 The Authors. Published by American Chemical Society

https://doi.org/10.1021/acscatal.3c00536
ACS Catal. 2023, 13, 5578−5583

chiral 1,5-diene structure bearing two orthogonal stereodefined functionalities (Scheme 1d). This high degree of functionalization would provide a useful tool to significantly expand the range of accessible molecules bearing the important and synthetically versatile 1,5-diene core.[14] Moreover, it would represent a new synthetic application among the few catalytic methods available for the stereoselective synthesis of acyclic alkenyl chlorides.[15]

The envisioned transformation is highly demanding since it requires a chemo-, regio-, and stereoselective Cu-Bpin addition to the allene, followed by a regio- and enantioselective coupling of the resulting allylcopper species with the allylic *gem*-dichloride in a process where the geometry of the alkenyl chloride must be also controlled. Here, we report the successful realization of this idea through an enantioselective copper-catalyzed borylative allyl−allyl cross-coupling between allenes and allylic *gem*-dichlorides that efficiently provides chiral, densely functionalized internal 1,5-dienes bearing both (*Z*)-configured alkenyl chloride and alkenyl boronate units with high levels of chemo-, regio-, and stereoselectivity.

We began our study by surveying the reaction between cyclohexylallene **1**, (*E*)-(3,3-dichloroprop-1-en-1-yl)benzene **2** and B_2pin_2 (Table 1).

Initial chiral ligand screening revealed that the use of catalysts bearing a chiral bisphosphine (entry 1) or amino-alcohol-derived *N*-heterocyclic carbene (NHC) ligands (entries 2−3) led to nearly equimolar mixtures of stereoisomers **3-*Z,Z*** and **3-*Z,E*** in low yield with almost negligible enantioselectivity. A significant improvement in stereoselectivity was observed when sulfonate-bearing NHC ligands[16] were employed. Chiral copper complexes derived from **L4** and **L5**, which feature a 2,6-dimethylphenyl and a mesityl group, respectively, proved to be the most efficient catalysts and provided 1,5-diene **3** as a single (*Z,Z*)-isomer with very good enantiomeric ratio (entries 4 and 5). Changes on the *N*-aryl group had a negative impact since bulkier substituents at the ortho position led to diminished enantioselectivity (entry 6), while a 3,5-disubstitution pattern produced a complete loss of efficiency (entry 7). Further evaluation of different solvents and reaction stoichiometry (entries 8−11) provided the optimal set of conditions, which comprises the use of **L5** as ligand, KO^{t}Bu as base, and toluene as solvent. Under these conditions, product **3** was obtained as a single isomer in 71% yield with 96:4 er (entry 11). Notably, no formation of other isomers arising either from coupling at the γ position of the allylcopper intermediate or from S_N2-type substitution of the allylic *gem*-dichloride could be detected. Interestingly, in sharp contrast with our previously reported borylative coupling between alkynes and allylic *gem*-dichlorides,[12] the use of alkoxide bases bearing smaller metal cations led to a significant decrease of both efficiency and stereoselectivity (entries 12−13).

Once the optimized conditions were identified, the scope of the reaction was explored (Scheme 2). The method proved to be remarkably effective for a wide range of allenes and provided solely the corresponding (*Z,Z*)-configured 1,5-dienes in good yield with excellent levels of chemo-, regio-, and enantioselectivity. Allenes bearing simple alkyl groups (**3**,**4**), or aliphatic chains bearing functionalities, such as aryl rings (**5**,**6**), silyl ether (**7**), ester (**8**), ether (**9**), or carbamate (**10**), were well tolerated. Heterocyclic-substituted allenes were also amenable for this transformation, as illustrated with the synthesis of piperidine and tetrahydropyran derivatives **11**

Table 1. Optimization Studies

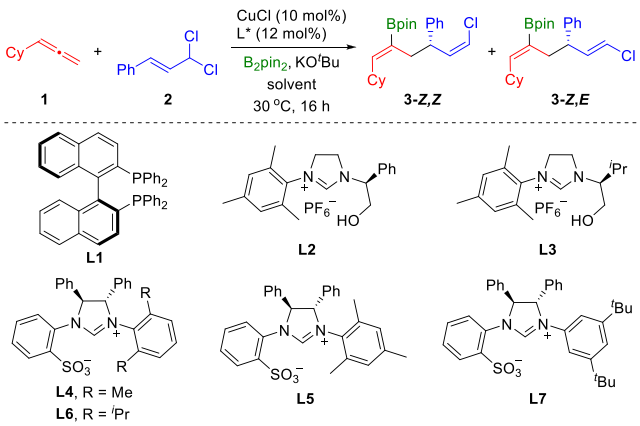

entry[a]	L*	solvent	conversion (%)[b]	Z,Z/Z,E ratio[c]	3 yield (%)[d]	3-(Z,Z/Z,E) er[e]
1	**L1**	THF	72	2.2:1	26	51:49/52:48
2	**L2**	THF	85	1.3:1	21	39:61/45:55
3	**L3**	THF	75	1.5:1	15	56:44/46:54
4	**L4**	THF	80	>20:1	34	93:7/-
5	**L5**	THF	90	>20:1	32	91:9/-
6	**L6**	THF	88	>20:1	24	52:48/-
7	**L7**	THF	70	-	-	-
8	**L4**	dioxane	full	>20:1	48	96:4/-
9[f,g]	**L4**	dioxane	full	>20:1	62	96:4/-
10[f,g]	**L5**	dioxane	full	>20:1	68	96:4/-
11[f,g]	**L5**	toluene	full	>20:1	71	96:4/-
12[f,g,h]	**L5**	toluene	full	20:1	36	90:10/72:28
13[f,g,i]	**L5**	toluene	full	5:1	32	77:23/56:44

[a]Reaction conditions: **1** (0.3 mmol), **2** (0.2 mmol), B_2pin_2 (0.32 mmol), CuCl (10 mol %), ligand (12 mol %), KO^{t}Bu (0.3 mmol), and solvent (2.0 mL) at 30 °C. [b]Conversion (**2** consumption) was determined by ^{1}H NMR analysis using an internal standard. [c]Determined by ^{1}H NMR analysis of reaction crude. [d]Yield of isolated product. [e]Enantioselectivity determined by SFC analysis. [f]Using 0.4 mmol of KO^{t}Bu. [g]Using 0.4 mmol of **1**. [h]NaO^{t}Bu used instead of KO^{t}Bu. [i]LiO^{t}Bu used instead of KO^{t}Bu.

and **12**. 1-Phenylallene still provided the corresponding product **13** as a single (*Z,Z*)-isomer with perfect regioselectivity, albeit with slightly diminished enantiomeric ratio.[17] Importantly, scalability of the reaction was demonstrated through the 1 mmol-scale synthesis of **3** using lower catalyst loading (5 mol %).

Different allylic *gem*-dichlorides were also evaluated for this enantioselective borylative allyl−allyl cross-coupling. Substrates with aryl rings bearing alkyl (**14**) or trifluoromethyl (**15**) groups proved to be efficient for this transformation. Halogenated aromatic substrates also furnished the corresponding 1,5-dienes (**16**−**19**) with good yield and excellent selectivities. Remarkably, the use of a hindered *ortho*-bromo-substituted substrate was well tolerated and provided products **18** and **19** without selectivity erosion. A substrate featuring another sterically demanding unit, such as a naphthalene group, could also be used with very high selectivity (**20**). Aliphatic *gem*-dichlorides were not suitable for the described enantioselective borylative allyl−allyl coupling.[18] Absolute stereochemistry of the products was determined by X-ray diffraction analysis of product **11**, which revealed the

https://doi.org/10.1021/acscatal.3c00536
ACS Catal. 2023, 13, 5578−5583

Scheme 2. Scope of the Enantioselective Borylative Coupling of Allenes and Allylic *gem*-Dichlorides[a]

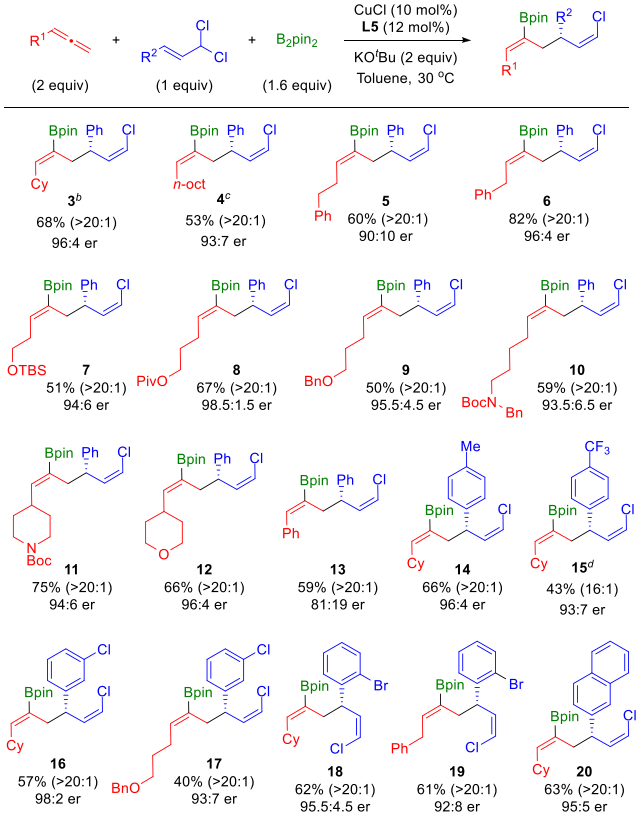

[a]Unless otherwise noted, all reactions were performed on a 0.2 mmol scale under optimized conditions (Table 1, entry 11). Yield values refer to isolated products. *Z,Z*/*Z,E* selectivity is reported in brackets. [b]Reaction run on a 1 mmol scale using 5 mol % of the catalyst. [c]Reaction run at 40 °C over 48 h. [d]Reaction run at 60 °C.

configuration of the carbon stereogenic center to be (*S*), and confirmed the (*Z*)-configuration of both double bonds.

The combination of the high level of functionality of the products and their stereochemistry makes them versatile building blocks for the synthesis of a range of chiral structures (Scheme 3). Stereodefined 1,5-dienyl chlorides **21** and **22** could be accessed by chemoselective intermolecular Suzuki–Miyaura cross-coupling. Because of the remaining alkenyl chloride, the 1,5-diene structure can be further functionalized as shown with the formation of **23**. The presence of an *ortho*-bromo-substituted aryl ring in products **18** and **19** provides an extra handle to perform an intramolecular coupling, as illustrated with the synthesis of indane derivative **24**. Notably, the alkenyl boronate and the alkenyl chloride functionalities could be efficiently combined through intramolecular Pd-catalyzed cross-coupling to provide chiral cyclopentene **25**. Oxidation of the alkenyl boronate unit allows for the preparation of chiral alkenyl chloride-containing ketones (i.e., **26–30**). Finally, chiral borylated 1,5-enyne **31** could be obtained with full stereochemical retention by LDA-mediated dehydrochlorination.

To analyze the factors that control the stereoselectivity of this enantioselective borylative allyl–allyl coupling, DFT calculations were performed (see the Supporting Information for details). Two lowest-energy structures (**Ia** and **Ib**), which rapidly interconvert (ΔG_{sol} = 0.5 kcal·mol^{-1}), were found for

Scheme 3. Synthetic Modifications of Products[a]

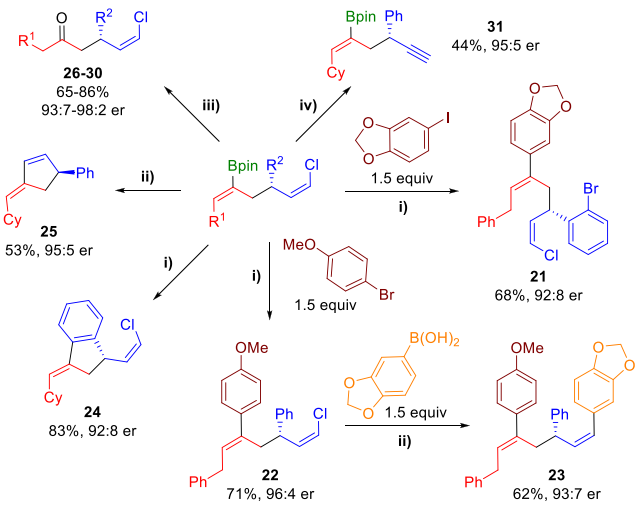

[a]Conditions: (i) $Pd(PPh_3)_4$ (10 mol %), NaOH 2M, dioxane, 100 °C; (ii) $Pd_2(dba)_3$ (5 mol %), XPhos (10 mol %), CsF (3 equiv), dioxane, 100 °C; (iii) $NaBO_3{\cdot}4H_2O$ (5 equiv), THF:H_2O, rt; (iv) LDA (2.5 equiv), THF, −78 °C, 5 min.

the σ-allyl-Cu(I) intermediate. Among the different investigated coordination modes for the stereodetermining oxidative addition step in the formation of **3-*Z,Z***,[19] the one featuring the allyl *gem*-dichloride opposite to the *N*-arylsulfonate group (i.e., coordination to **Ia**), led to the most favorable pathway to the major (*S*)-enantiomer, while the preferred pathway to the minor (*R*)-enantiomer arises from coordination to **Ib** where the allyl substrate is opposite to the *N*-mesityl (NMes) unit (Figure 1a). The relative energy for transition state **TS$_{OA}$-*Z,S*** was 2.7 kcal·mol^{-1} lower than for **TS$_{OA}$-*Z,R***, which is in good agreement with the observed 96:4 er. In order to account for this energy difference, analysis of non-covalent interactions (NCI) was performed. NCI plots of both transition state structures showed no significant differences in terms of repulsive interactions (see the Supporting Information). However, analysis of the attractive interactions revealed that the coordination mode in **TS$_{OA}$-*Z,S*** allows for the establishment of a double potassium cation bridge interaction between the NHC's sulfonate group and both chloride units. In contrast, only one K···Cl interaction is present in **TS$_{OA}$-*Z,R*** (Figure 1b). This difference in attractive interactions may suggest that the origin of enantioselectivity arises from the extra stabilization in **TS$_{OA}$-*Z,S***, which originates from the double substrate–ligand cation bridge interaction. In this line, analysis of the optimized structures for the transition states using a lithium cation instead of potassium showed that the extra stabilization given by the second cation bridge interaction of the second chlorine atom is missing in **TS$_{OA}$-*Z,S*-Li** (Figure 1c). This leads to a higher-energy transition state and, thus, to a smaller energy difference with **TS$_{OA}$-*Z,R*-Li**.[20] The lack of the second stabilizing interaction may be due to the smaller size of the Li cation and might explain the lower enantioselectivity observed when LiO^{t}Bu is used instead of KO^{t}Bu (see Table 1, entries 11 vs 13).

To evaluate the factors that govern the diastereoselective formation of the (*Z*)-alkenyl chloride, we calculated the optimized structure for transition state **TS$_{OA}$-*E,S*** that leads to the formation of diastereomer **3-*Z,E***.[21] In accordance with the experimental results, **TS$_{OA}$-*E,S*** resulted in higher energy than

https://doi.org/10.1021/acscatal.3c00536
ACS Catal. 2023, 13, 5578−5583

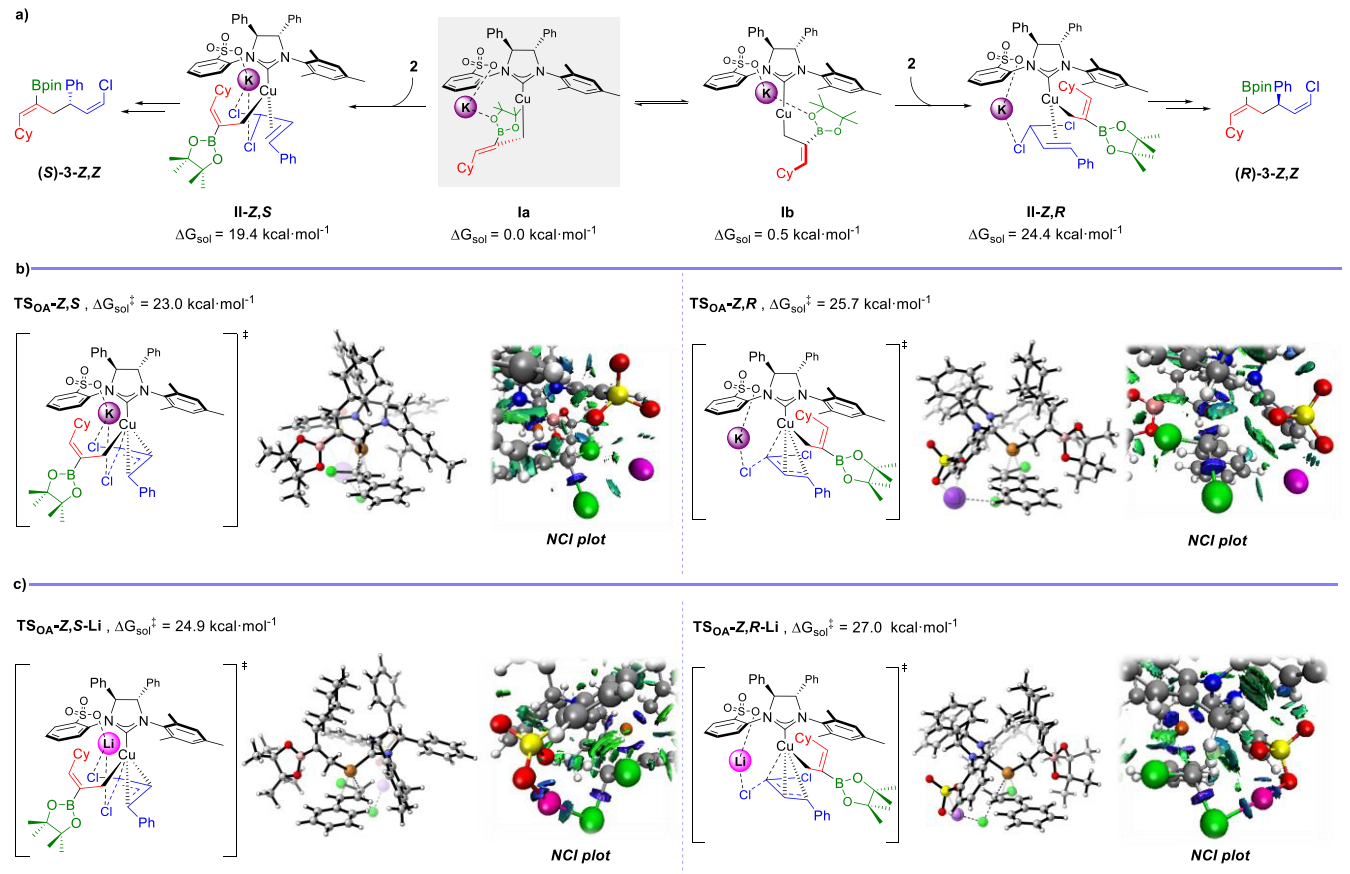

Figure 1. Optimized structures and energies obtained from DFT calculations performed at the ωB97XD/*def*2-TZVP/*def*2-QZVP (Cu) (scrf = smd, toluene)//ωB97XD/6-31G(d,p)/SDD+f (Cu) level for (a) σ-allyl-Cu(I) intermediates **Ia** and **Ib** and their most favorable π-olefin Cu(I) complexes with allylic *gem*-dichloride **2** and for (b) the stereochemistry-determining oxidative-addition transition states associated with the most favored pathways leading to (*S*)-3,*Z*,*Z* and (*R*)-3,*Z*,*Z* using KO^{t}Bu and (c) using LiO^{t}Bu.

the preferred **TS$_{OA}$-*Z*,*S*** ($\Delta G^{\ddagger}$ = 30.7 kcal·mol^{-1} vs $\Delta G^{\ddagger}$ = 23.0 kcal·mol^{-1}). NCI plot analysis revealed that a new repulsive interaction between the Bpin unit and the *N*-arylsulfonate group appears in **TS$_{OA}$-*E*,*S*** when compared with **TS$_{OA}$-*Z*,*S*** (Figure 2). Moreover, repulsive interactions between the cyclohexyl ring and the phenyl and NMes units of the NHC ligand become larger in **TS$_{OA}$-*E*,*S***. Analysis of **TS$_{OA}$-*E*,*S*** geometry shows that in order to establish the stabilizing double-cation bridge interaction the system has to adopt a structural reorganization, which involves a decrease on the dihedral angle displayed between NHC carbenic carbon and C6 of the arylsulfonate ring (60.5° in **TS$_{OA}$-*E*,*S*** vs 68.2° in **TS$_{OA}$-*Z*,*S***). This angle modification pushes the *N*-arylsulfonate ring closer to the Bpin unit, thereby engendering the new repulsive interaction. Consequently, the σ-allyl substituent adopts a new spatial disposition that enhances the repulsive interactions between the cyclohexyl group and the NHC's phenyl and mesityl rings. This set of repulsive interactions would result in a higher-energy transition state and would explain the origin of the (*Z*)-selectivity.

In summary, we have disclosed an enantioselective borylative allyl−allyl cross-coupling between allenes and allylic *gem*-dichlorides to provide optically active (*Z*,*Z*)-configured internal 1,5-dienes. Remarkable features of the method are the observed excellent chemo-, regio-, and enantioselectivity, the stereoselective formation of two orthogonally functionalized alkenyl units, and the synthetic versatility of the resulting chiral

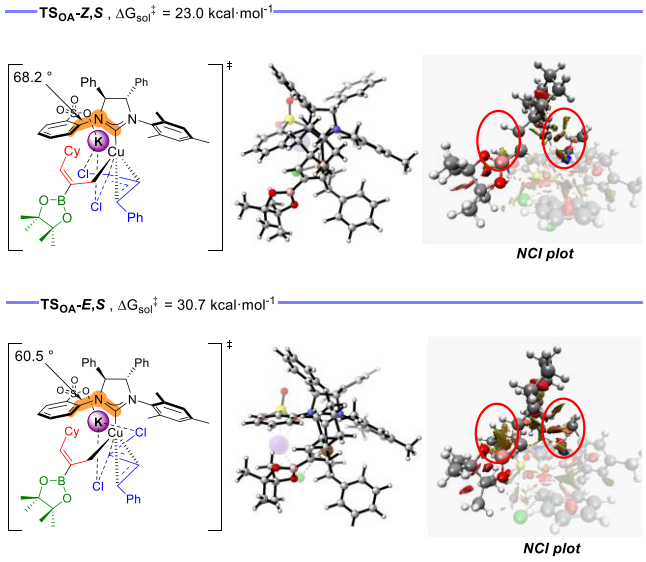

Figure 2. Optimized structures and energies obtained from DFT calculations performed at the ωB97XD/*def*2-TZVP/*def*2-QZVP (Cu) (scrf = smd, toluene)//ωB97XD/6-31G(d,p)/SDD+f (Cu) level for stereochemistry-determining oxidative-addition transition states associated with the most favored pathways leading to (*S*)-3,*Z*,*Z* and (*S*)-3,*Z*,*E*.

https://doi.org/10.1021/acscatal.3c00536
ACS Catal. 2023, 13, 5578−5583

borylated chlorodienes. Intrinsic stereochemical features were analyzed by DFT calculations, which revealed key noncovalent interactions that allow rationalization of the observed high levels of enantio- and diastereoselectivity.

■ ASSOCIATED CONTENT

Supporting Information

The Supporting Information is available free of charge at https://pubs.acs.org/doi/10.1021/acscatal.3c00536.

List of starting materials and ligands, experimental procedures, compound characterization data, NMR spectra, X-ray crystallographic data for **11**, details for DFT calculations, NCI plots, Cartesian coordinates, imaginary frequencies, and absolute energies in hartrees for all optimized geometries (PDF)

CCDC 2222779 (CIF)

Accession Codes

CCDC 2222779 contains the supplementary crystallographic data for this paper. These data can be obtained free of charge via www.ccdc.cam.ac.uk/data_request/cif, or by emailing data_request@ccdc.cam.ac.uk, or by contacting The Cambridge Crystallographic Data Centre, 12 Union Road, Cambridge CB2 1EZ, UK; fax: + 44 1223 336033.

■ AUTHOR INFORMATION

Corresponding Author

Martín Fañanás-Mastral − *Centro Singular de Investigación en Química Biolóxica e Materiais Moleculares (CiQUS), Universidade de Santiago de Compostela, 15782 Santiago de Compostela, Spain;* orcid.org/0000-0003-4903-0502; Email: martin.fananas@usc.es

Authors

Martín Piñeiro-Suárez − *Centro Singular de Investigación en Química Biolóxica e Materiais Moleculares (CiQUS), Universidade de Santiago de Compostela, 15782 Santiago de Compostela, Spain*

Andrés M. Álvarez-Constantino − *Centro Singular de Investigación en Química Biolóxica e Materiais Moleculares (CiQUS), Universidade de Santiago de Compostela, 15782 Santiago de Compostela, Spain;* orcid.org/0000-0001-8948-1258

Complete contact information is available at: https://pubs.acs.org/10.1021/acscatal.3c00536

Notes

The authors declare no competing financial interest.

■ ACKNOWLEDGMENTS

Financial support from the AEI (PID2020-118237RB-I00), European Research Council (863914), Xunta de Galicia (ED431C 2022/27; Centro singular de investigación de Galicia accreditation 2019-2022, ED431G 2019/03), and the European Regional Development Fund (ERDF) is gratefully acknowledged. M.P.-S. and A.M.A.-C. thank AEI and Xunta de Galicia, respectively, for predoctoral fellowships. We also thank the use of RIAIDT-USC analytical facilities and CESGA (Xunta de Galicia) for computational time.

■ REFERENCES

(1) (a) *Catalytic Asymmetric Synthesis*; Ojima, I., Ed.; Wiley: Hoboken, NJ, 2010. (b) de Graaff, C.; Ruijter, E.; Orru, R. V. A. Recent developments in asymmetric multicomponent reactions. *Chem. Soc. Rev.* **2012**, *41*, 3969−4009.

(2) (a) Zhang, P.; Brozek, L. A.; Morken, J. P. Pd-Catalyzed Enantioselective Allyl−Allyl Cross-Coupling. *J. Am. Chem. Soc.* **2010**, *132*, 10686−10688. (b) Zhang, P.; Le, H.; Kyne, R. E.; Morken, J. P. Enantioselective Construction of All-Carbon Quaternary Centers by Branch-Selective Pd-Catalyzed Allyl−Allyl Cross-Coupling. *J. Am. Chem. Soc.* **2011**, *133*, 9716−9719. (c) Brozek, L. A.; Ardolino, M. J.; Morken, J. P. Diastereocontrol in Asymmetric Allyl−Allyl Cross-Coupling: Stereocontrolled Reaction of Prochiral Allylboronates with Prochiral Allyl Chlorides. *J. Am. Chem. Soc.* **2011**, *133*, 16778−16781. (d) Ardolino, M. J.; Morken, J. P. Congested C−C Bonds by Pd-Catalyzed Enantioselective Allyl−Allyl Cross-Coupling, a Mechanism-Guided Solution. *J. Am. Chem. Soc.* **2014**, *136*, 7092−7100. (e) Wang, X.; Wang, X.; Han, Z.; Wang, Z.; Ding, K. Palladium-Catalyzed Asymmetric Allylic Allylation of Racemic Morita-Baylis-Hillman Adducts. *Angew. Chem., Int. Ed.* **2017**, *56*, 1116−1119.

(3) (a) Hornillos, V.; Pérez, M.; Fañanás-Mastral, M.; Feringa, B. L. Copper-Catalyzed Enantioselective Allyl−Allyl Cross-Coupling. *J. Am. Chem. Soc.* **2013**, *135*, 2140−2143. (b) Yasuda, Y.; Ohmiya, H.; Sawamura, M. Copper-Catalyzed Enantioselective Allyl-Allyl Coupling between Allylic Boronates and Phosphates with a Phenol/N-Heterocyclic Carbene Chiral Ligand. *Angew. Chem., Int. Ed.* **2016**, *55*, 10816−10820.

(4) (a) Hamilton, J. Y.; Hauser, N.; Sarlah, D.; Carreira, E. M. Iridium-Catalyzed Enantioselective Allyl-Allylsilane Cross-Coupling. *Angew. Chem., Int. Ed.* **2014**, *53*, 10759−10762. (b) Zheng, Y.; Yue, B.-B.; Wei, K.; Yang, Y.-R. Iridium-Catalyzed Enantioselective Allyl−Allyl Cross-Coupling of Racemic Allylic Alcohols with Allylboronates. *Org. Lett.* **2018**, *20*, 8035−8038.

(5) To the best of our knowledge, the only example of an asymmetric allyl−allyl coupling that provides acyclic internal 1,5-dienes is based on a stereospecific allyl−allyl coupling involving chirality transfer from enantioenriched internal allylic electrophiles: Le, H.; Batten, A.; Morken, J. P. Catalytic Stereospecific Allyl−Allyl Cross-Coupling of Internal Allyl Electrophiles with AllylB(pin). *Org. Lett.* **2014**, *16*, 2096−2099.

(6) For two examples of allyl−allyl cross-coupling involving cyclic allyl electrophiles with moderate enantioselectivity, see ref 3b. For a stereospecific allyl−allyl cross-coupling between an enantioenriched piperidinyl allylic boronate and allylic carbonates, see: Estaitie, M.; Hall, D. G. Regiocontrolled synthesis of enantioenriched 2-substituted dehydropiperidines by stereospecific allyl−allyl cross-coupling of a chiral allylic boronate. *Chem. Commun.* **2022**, *58*, 1370−1373.

(7) (a) Pulis, A. P.; Yeung, K.; Procter, D. J. Enantioselective copper catalysed, direct functionalisation of allenes via allyl copper intermediates. *Chem. Sci.* **2017**, *8*, 5240−5247. (b) Fujihara, T.; Tsuji, Y. Cu-Catalyzed Borylative and Silylative Transformations of Allenes: Use of β-Functionalized Allyl Copper Intermediates in Organic Synthesis. *Synthesis* **2018**, *50*, 1737−1749. (c) Whyte, A.; Torelli, A.; Mirabi, B.; Zhang, A.; Lautens, M. Copper-Catalyzed Borylative Difunctionalization of π-Systems. *ACS Catal.* **2020**, *10*, 11578−11622.

(8) Meng, F.; McGrath, K. P.; Hoveyda, A. H. Multifunctional organoboron compounds for scalable natural product synthesis. *Nature* **2014**, *513*, 367−374.

(9) Xu, G.; Fu, B.; Zhao, H.; Li, Y.; Zhang, G.; Wang, Y.; Xiong, T.; Zhang, Q. Enantioselective and site-specific copper-catalyzed reductive allyl−allyl cross-coupling of allenes. *Chem. Sci.* **2019**, *10*, 1802−1806.

(10) Sun, Y.; Zhou, Y.; Shi, Y.; del Pozo, J.; Torker, S.; Hoveyda, A. H. Copper−Hydride-Catalyzed Enantioselective Processes with Allenyl Boronates. Mechanistic Nuances, Scope, and Utility in Target-Oriented Synthesis. *J. Am. Chem. Soc.* **2019**, *141*, 12087−12099.

(11) Semba, K.; Bessho, N.; Fujihara, T.; Terao, J.; Tsuji, Y. Copper-Catalyzed Borylative Allyl-Allyl Coupling Reaction. *Angew. Chem., Int. Ed.* **2014**, *53*, 9007−9011.

(12) Chaves-Pouso, A.; Álvarez-Constantino, A. M.; Fañanás-Mastral, M. Enantio- and Diastereoselective Copper-Catalyzed Allylboration of Alkynes with Allylic gem-Dichlorides. *Angew. Chem., Int. Ed.* **2022**, *61*, e202117696.

(13) For a copper-catalyzed enantioselective allylic substitution of allyl *gem*-dichlorides with alkyl Grignard reagents, see: Giannerini, M.; Fañanás-Mastral, M.; Feringa, B. L. Z-Selective Copper-Catalyzed Asymmetric Allylic Alkylation with Grignard Reagents. *J. Am. Chem. Soc.* **2012**, *134*, 4108−4111.

(14) (a) Breitmaier, E. *Terpenes: Flavors, Fragrances, Pharmaca, Pheromones*; Wiley-VCH: Weinheim, Germany, 2006. . (b) Felix, R. J.; Weber, D.; Gutierrez, O.; Tantillo, D. J.; Gagné, M. R. A gold-catalysed enantioselective Cope rearrangement of achiral 1,5-dienes. *Nat. Chem.* **2012**, *4*, 405−409. and references therein.

(15) Koh, M. J.; Nguyen, T. T.; Zhang, H.; Schrock, R. R.; Hoveyda, A. H. Direct synthesis of Z-alkenyl halides through catalytic cross-metathesis. *Nature* **2016**, *531*, 459−465.

(16) For a review on the use of chiral sulfonate-bearing NHC-Cu complexes in enantioselective catalysis, see: (a) Hoveyda, A. H.; Zhou, Y.; Shi, Y.; Brown, M. K.; Wu, H.; Torker, S. Sulfonate N-Heterocyclic Carbene−Copper Complexes: Uniquely Effective Catalysts for Enantioselective Synthesis of C−C, C−B, C−H, and C−Si Bonds. *Angew. Chem., Int. Ed.* **2020**, *59*, 21304−21359. For selected examples, see: (b) Gao, F.; Carr, J. L.; Hoveyda, A. H. A Broadly Applicable NHC−Cu-Catalyzed Approach for Efficient, Site-, and Enantioselective Coupling of Readily Accessible (Pinacolato)-alkenylboron Compounds to Allylic Phosphates and Applications to Natural Product Synthesis. *J. Am. Chem. Soc.* **2014**, *136*, 2149−2161. (c) Shi, Y.; Jung, B.; Torker, S.; Hoveyda, A. H. N-Heterocyclic Carbene−Copper-Catalyzed Group-, Site-, and Enantioselective Allylic Substitution with a Readily Accessible Propargyl(pinacolato)-boron Reagent: Utility in Stereoselective Synthesis and Mechanistic Attributes. *J. Am. Chem. Soc.* **2015**, *137*, 8948−8964. (d) Xu, G.; Zhao, H.; Fu, B.; Cang, A.; Zhang, G.; Zhang, Q.; Xiong, T.; Zhang, Q. Ligand-Controlled Regiodivergent and Enantioselective Copper-Catalyzed Hydroallylation of Alkynes. *Angew. Chem., Int. Ed.* **2017**, *56*, 13130−13134. (e) Zhou, Y.; Shi, Y.; Torker, S.; Hoveyda, A. H. S_N2''-Selective and Enantioselective Substitution with Unsaturated Organo-boron Compounds and Catalyzed by a Sulfonate-Containing NHC-Cu Complex. *J. Am. Chem. Soc.* **2018**, *140*, 16842−16854. (f) Rivera-Chao, E.; Mitxelena, M.; Varela, J. A.; Fañanás-Mastral, M. Copper-Catalyzed Enantioselective Allylboration of Alkynes: Synthesis of Highly Versatile Multifunctional Building Blocks. *Angew. Chem., Int. Ed.* **2019**, *58*, 18230−18234.

(17) Although the reason for this difference in enantioselectivity is not yet clear, π interactions between the phenyl group coming from the allene and the ligand may account for the lower enantioselectivity observed for this allene.

(18) Aliphatic *gem*-dichlorides provided the corresponding internal 1,5-dienes with excellent (*Z*)-selectivity, although with low enantioselectivity. See the Supporting Information for details.

(19) Reductive elimination from π-allyl-Cu(III) intermediate to final coordinated products was found to be lower in energy than the oxidative addition step. For the whole reaction energy profile, see the Supporting Information.

(20) The energy difference between calculated transition states for the Li cation system ($\Delta\Delta G^{\ddagger}$ = 2.1 kcal·mol^{-1}) represents a 1.4 kcal·mol^{-1} overestimation compared with the experimental derived value ($\Delta\Delta G^{\ddagger}$ = 0.7 kcal·mol^{-1}, 77:23 er). Although a bit high, this difference is within the 1−2 kcal·mol^{-1} error that is typically considered sufficient for reaction energies: Bursch, M.; Mewes, J.-M.; Hansen, A.; Grimme, S. Best-Practice DFT Protocols for Basic Molecular Computational Chemistry. *Angew. Chem., Int. Ed.* **2022**, *61*, e202205735.

(21) The optimized structure for transition state $\mathbf{TS_{OA}}$-***E,S*** that leads to diastereomer (***R***)-3-***Z,E*** was also calculated and features an even higher relative energy than $\mathbf{TS_{OA}}$-***E,S***. See the Supporting Information for details.

https://doi.org/10.1021/acscatal.3c00536
ACS Catal. 2023, 13, 5578−5583